TITLE: **Preliminary evaluation of the impact of temperature fluctuations in the HFI 4K-stage on LFI**

DOC. TYPE: TECHNICAL NOTE

PROJECT REF.: PL-LFI-PST-TN-048 **PAGE:** I of IV, 10

ISSUE/REV.: Issue 2.0 **DATE:** June 2006

Prepared by	L. TERENZI A. MENNELLA G. MORGANTE M. TOMASI L. VALENZIANO LFI System Team	Date: Signature:	June 6th, 2006 [signatures]
Agreed by	C. BUTLER LFI Program Manager	Date: Signature:	June 6th, 2006 [signature]
Approved by	N. MANDOLESI LFI Principal Investigator	Date: Signature:	June 6th, 2006 [signature]

DISTRIBUTION LIST

Recipient	Company / Institute	E-mail address
T. PASSVOGEL	ESA – Noordwijk	tpassvog@estec.esa.nl
G. CRONE	ESA – Noordwijk	Gerald.Crone@esa.int
J. MARTI-CANALES	ESA – Noordwijk	Javier.Marti.Canales@esa.int
J. TAUBER	ESA – Noordwijk	Jan.Tauber@esa.int
J. RAUTAKOSKI	ESA – Noordwijk	Jan.Rautakoski@esa.int
B. COLLAUDIN	ALCATEL – Cannes	bernard.collaudin@space.alcatel.fr
J.P. CHAMBELLAND	ALCATEL – Cannes	Jean-Philippe.Chambelland@space.alcatel.fr
N. MANDOLESI	IASF/INAF – Bologna	mandolesi@iasfbo.inaf.it
C. BUTLER	IASF/INAF – Bologna	butler@iasfbo.inaf.it
G. MORGANTE	IASF/INAF – Bologna	morgante@iasfbo.inaf.it
L. STRINGHETTI	IASF/INAF – Bologna	stringhetti@iasfbo.inaf.it
F. VILLA	IASF/INAF – Bologna	villa@iasfbo.inaf.it
M. BERSANELLI	UNIMI – Milano	Marco.bersanelli@mi.infn.it
D. MENNELLA	UNIMI – Milano	Aniello.Mennella@fisica.unimi.it
M. TOMASI	IASF/INAF – Milano	tomasi@lambrate.inaf.it
M. MICCOLIS	ALENIA SPAZIO – LABEN	Maurizio.Miccolis.m@aleniaspazio.it
R. SILVESTRI	ALENIA SPAZIO – LABEN	Roberto.Silvestri@aleniaspazio.it
P. LEUTENEGGER	ALENIA SPAZIO – LABEN	Paolo.Leutenegger@aleniaspazio.it
4KRL Team - Bologna	INAF/IASF – Bologna	
C. LAWRENCE	JPL – Pasadena	crl@jplsp.jpl.nasa.gov
T. GAIER	JPL – Pasadena	gaier@merlin.jpl.nasa.gov
M. SEIFFERT	JPL – Pasadena	Michael.d.seiffert@jpl.nasa.gov
J.L. PUGET	IAS – Orsay	puget@ias.u-psud.fr
J-M. LAMARRE	LERMA – Paris	lamarre@ias.u-psud.fr
J-J. FOURMOND	IAS – Orsay	fourmond@ias.u-psud.fr
S. VARESI	IAS – Orsay	sylvain.varesi@ias.u-psud.fr
J. FEREDAY	RAL – Chilton (UK)	j.fereday@rl.ac.uk
R. EMERY	RAL – Chilton (UK)	r.j.emery@rl.ac.uk
LFI SPCC	IASF/INAF – Bologna	lfispcc@iasfbo.inaf.it

CHANGE RECORD

Issue	Date	Sheet	Description of Change	Release
Issue 1.0	Sept '03	All	First issue of document	1.0
Issue 2.0	Jun '06	All	New datasets used for all the estimation	2.0

Table of Content

Abstract

In this technical note we provide a preliminary analysis of the effect of temperature fluctuations at the level of the HFI 4K stage on the scientific performances of the Planck-LFI instrument. The stability of this stage is of crucial importance for the LFI, as it impact directly the stability of the measured signal through its reference load. The availability of the first simulations of the 4K temperature stability from the HFI team has prompted a quick assessment of the expected effect, which is found to be large enough to require the application of software removal algorithms to maintain the residual effect in the final maps within the required levels. Clearly it is of crucial importance the availability in a short time of measurements from the HFI 4K cooler in order to be able to perform robust estimates of the final expected systematic effect.

1. Introduction

The Planck-LFI radiometric receivers are pseudo-correlation radiometers [1, 2] that continuously compare the sky signal with a stable reference signal in order to minimise the effects from gain instabilities. This reference signal is provided by ECCOSORB loads thermally linked to the HFI 4K stage [3] which must display a high degree of stability to maintain at a μK level in the final maps any spurious signal caused by such instabilities.

1.1 4K Reference Load Implementation

70 GHz loads are mounted on the upper part of the HFI cryostat. They are bonded to a mounting structure facing the 6 LFI 70 GHz FEMs. 30 and 44 GHz loads are located on the cylindrical part of the HFI cryostat. They are mounted in individuals mounting structures. These latter loads are closer to the 4K cooler cold end and are the most affected by temperature fluctuations, in particular after the implementation of a PID temeprature control on the HFI focal plane.

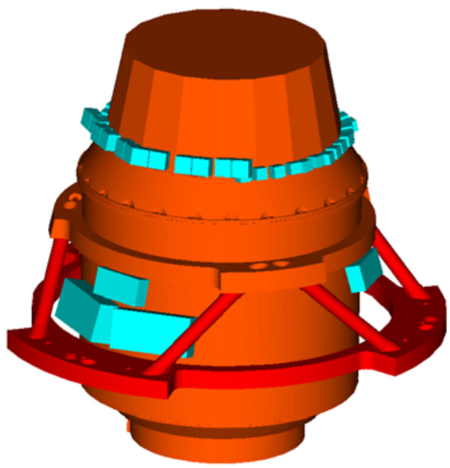

Figure 1 –Loads location on the HFI cryostat. Small blue blocks on the upper sector (100 GHz loads) are

not present anymore

1.2 Temperature stability requirements

The stability requirements of the reference load temperature have been specified in [4] and are summarised in the table below:

Table 1 – Required stability of the temperature of the LFI 4K reference loads

Random fluctuations (high frequencies, > 1 Hz)	Spin-synchronous fluctuations	Periodic fluctuations (non spin-synchronous, low frequencies < 1 Hz)
10 mK/Hz$^{1/2}$	± 1 μK	± 1 mK

The temperature stability at the level of the reference loads is the result of temperature fluctuations propagating from many sources through the HFI instrument to the loads located on the external shield of the HFI box:

- temperature fluctuations at the LR2/LFI interface that propagate to the HFI instrument through the struts connecting the HFI to the LFI;
- temperature fluctuations at the LR1/HFI interface propagating from the 18 K plate to the 4 K cold end;
- temperature fluctuations at the 4 K cold end propagating through the 4 K box to the LFI reference loads.

Furthermore we must take into account that the temperature stability of the various cold ends are not independent; in fact the stability of the LR1 cold end depends on the stability of the LR2 cold end and the stability of the 4 K cooler itself depends on the stability of the temperature of the 18 K stage.

The HFI team has made available estimations of the temperature stability at some interface points between the 4 K box and the reference loads considering the temperature behaviour of the LR1 cold end. This behaviour has been derived from the latest tests on the FM2 Sorption Cooler in which a PID active control was implemented to stabilise the temperature at the LR2/LFI interface. The propagation of the resulting temperature oscillations through the ECCOSORB targets has been measured during the QM test campaign. In this note we report preliminary estimations of the effect of such temperature instabilities.

The results show that the effect is going to be kept under control within the requirements. Further investigations are needed (i) to evaluate the effect of temperature fluctuations of the 4K cooler itself, (ii) to evaluate the effect on maps and power spectra also considering the presence of various astrophysical signals and instrumental noises, and (iii) to model more accurately the signal emitted by the reference load into the radiometer as a consequence of physical temperature fluctuations.

2. Sources of thermal instability

In this study only the sorption cooler cold-ends LR1 and LR2 have been considered as sources of temperature oscillations. Therefore the temperature fluctuations at the level of the 4 K cooler neglect any possible contribution from instabilities intrinsic to the 4 K cooler itself. The input data of temperature versus time at the 18 K and 20 K stages come from a set of measurements performed on the Sorption Cooler FM2 in which the LR2/LFI interface was stabilized with an active PID controller. For further informations regarding the controller implementation see [5, 6].

In **Figure 2** we show the measured temperature at the LR1 cold end while in **Figure 3** we report the corresponding amplitude spectra.

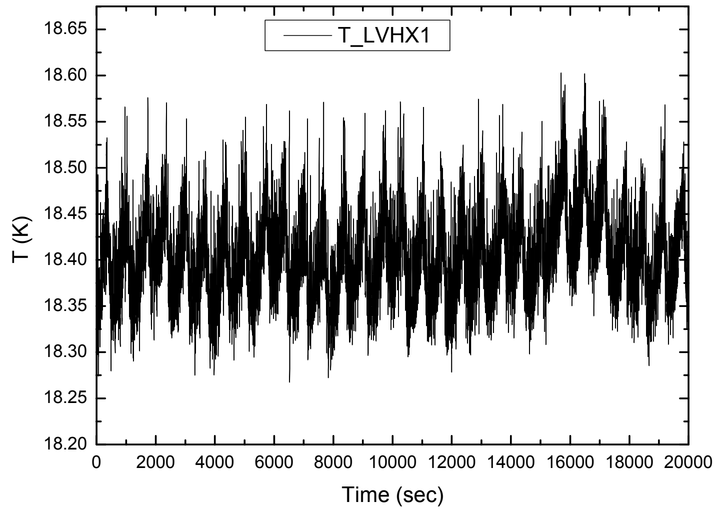

Figure 2 – Temperature at the LR1 cold end of the FM2 Sorption Cooler

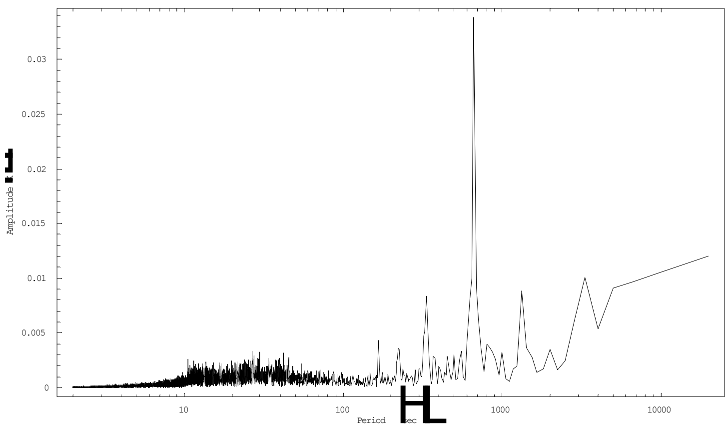

Figure 3 – Amplitude spectrum of the temperature fluctuations at the LR1 cold end of the FM2 Sorption Cooler

3. Propagation of temperature fluctuations from LR1 to the LFI reference loads

In [7] it has been reported a thermal simulation study with the aim to evaluate the transfer function (f_{trans}) characterising the propagation of temperature fluctuations from the LR1 cold end to the 4 K box, which was then verified in November 2004 calibration tests. The transfer function is such that for each position $\vec{x}$ on the 4 K box the amplitude of a temperature fluctuation having frequency ν and phase ϕ can be calculated as:

$$\Delta T(\vec{x}, \nu, \phi) = f_{\mathrm{trans}}(\vec{x}, \nu, \phi) \times \Delta T_{\mathrm{LR1}}(\nu, \phi) \qquad (1)$$

In Figure 4 we show both the amplitude transfer function relative to a 30 GHz and 70 GHz channel reference loads, which represents the worst and best cases (see discussion in Sec.1.1). In our treatment we have neglected the phase contribution to the transfer function, as it was not evaluated in the HFI study.

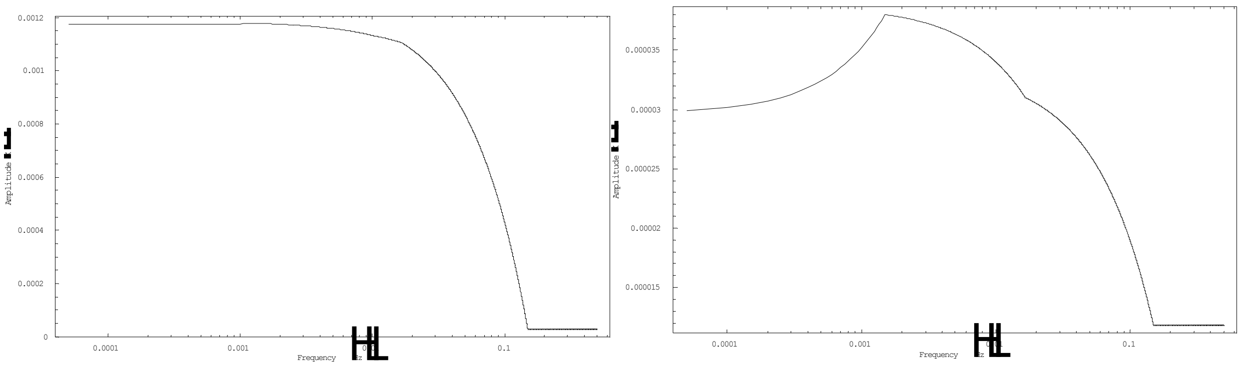

Figure 4 – Amplitude transfer function for the propagation of temperature fluctuations from the LR1 cold end to the reference load at level of 30 and 44 GHz channels (left plot) and 70 GHz channel (right plot). The functions are different due to the greater effect of the PID stage on the 70 GHz, closer to HFI FPU.

We have also evaluated the thermal damping from the dedicated tests during the QM test campaign [8]; in Figure 5 we show the result relative to a 30 GHz target, which shows that the thermal damping provided by the loads themselves is negligible compared to the overall thermal damping (cfr. with Figure 4).

In this analysis, for the 70 GHz channel case, we used as a worst case the temperature curves at the interface between HFI and the reference load which is sufficient for reaching the requirement.

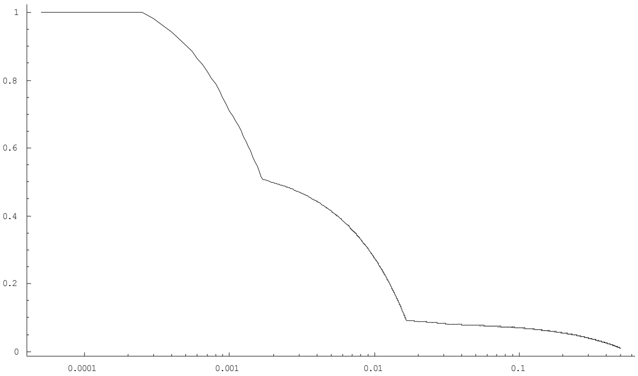

Figure 5 – Amplitude transfer function for the propagation of temperature fluctuations through a 30 GHz LFI reference load.

4. Measured signal instability

The next step is to convert the physical temperature fluctuation of the reference target first into a variation of the radiometer reference signal and ultimately into a variation of the measured signal.

Assuming perfect emissivity for the reference target we can approximate the variation of the reference signal in antenna temperature, ΔT_A caused by a variation in physical temperature, $\Delta T_{\rm phys}$, by $\Delta T_A = \frac{x^2 e^x}{\left(e^x - 1\right)^2}\delta T_{\rm phys} \equiv \eta \times \delta T_{\rm phys}$, where $x = \frac{h\nu}{kT_0}$ and, in our case, $T_0 \sim 4.5$ K.

The radiometric transfer function can be calculated considering the differential radiometer output power defined as:

$$p(t) = ak\beta G_{\rm FE} G_{\rm BE} G_{\rm DC}\left[\widetilde{T}_{\rm sky} + T_{\rm n_{FE}} + \frac{T_{\rm n_{BE}}}{G_{\rm FE}} - r\left(\widetilde{T}_{\rm 4K} + T_{\rm n_{FE}} + \frac{T_{\rm n_{BE}}}{G_{\rm FE}}\right)\right] \quad (2)$$

where:

- $\widetilde{T}_{\rm sky} = \frac{T_{\rm sky}}{L_{\rm feed-OMT}} + \left(1 - \frac{1}{L_{\rm feed-OMT}}\right)T_{\rm phys}$ represents the sky signal at the output of the feed-OMT system,
- $\widetilde{T}_{\rm 4K} = \frac{T_{\rm 4K}}{L_{\rm 4K}} + \left(1 - \frac{1}{L_{\rm 4K}}\right)T_{\rm phys}$ represents the reference signal at the output of the reference horns,
- $T_{\rm phys}$ is the temperature of the front end (~20 K),

- the L parameters represent the insertion losses of the front-end passive components,
- the G parameters represent gains of the RF and DC amplifiers,
- the T_n parameters represent the front-end and back-end amplifier noise temperatures,
- $r \approx \frac{\tilde{T}_{\rm sky} + T_{\rm sys}}{\tilde{T}_{\rm 4K} + T_{\rm sys}}$ is the gain modulation factor,
- β is the radiometer bandwidth, k the Boltzmann constant and a is the proportionality constant of the square law detectors.

In Table 2 we summarise the baseline radiometer parameters used in our calculations.

Table 2 – Baseline radiometer parameters

Frequency (GHz)	30	44	70
η	0.991513	0.98185	0.95482
$L_{\rm feed\text{-}OMT}$ (dB)	0.25	0.25	0.25
$L_{\rm 4K}$ (dB)	0.2	0.2	0.2
$G_{\rm FE}$(dB)	35	35	35
$G_{\rm BE}$(dB)	35	35	35
$T_{n_{\rm FE}}$(K)	8.60	14.10	25.70
$T_{n_{\rm BE}}$(K)	350	350	450
$T_{\rm phys}$(K)	20	20	20
r	0.8235	0.8721	0.9214

If we denote with $\delta T_{\rm rad}^{\rm 4K}$ the variation in the radiometer output caused by a variation $\delta T^{\rm 4K}$ in the reference load signal we can write $\delta T_{\rm rad}^{\rm 4K} = TF_{\rm rad}^{\rm 4K} \cdot \delta T^{\rm 4K}$ where $TF_{\rm rad}^{\rm 4K} = \left(\frac{\partial p}{\partial T_{\rm sky}}\right)^{-1} \frac{\partial p}{\partial T_{\rm 4K}} \delta T^{\rm 4K} = -r \frac{L_{\rm feed-OMT}}{L_{\rm 4K}}$.

In Figure 6 we show an example of the differential output of a 30 GHz radiometer caused by a fluctuation in the reference signal induced by temperature oscillations at the LR1 cold end (coupled scenario, see **Figure 2-**a). The peak-to-peak effect at this level is of the order of ~ 0.15 mK.

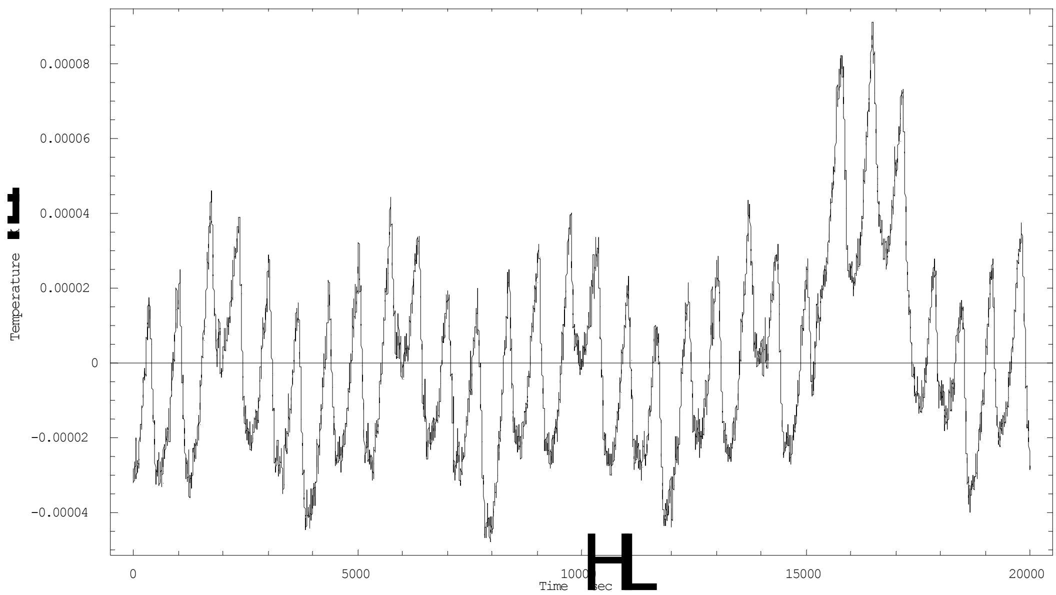

Figure 6. Time ordered data representing the 30 GHz radiometric output caused by a fluctuation in the 4K reference signal induced by LR1 temperature variations.

In Figure 7 we show the amplitude spectrum of the above data stream, from which it is apparent that the fluctuation is dominated by slow harmonics (with frequency < 1 mHz). In particular the right panel shows that the spin synchronous components are expected to be at sub-μK level.

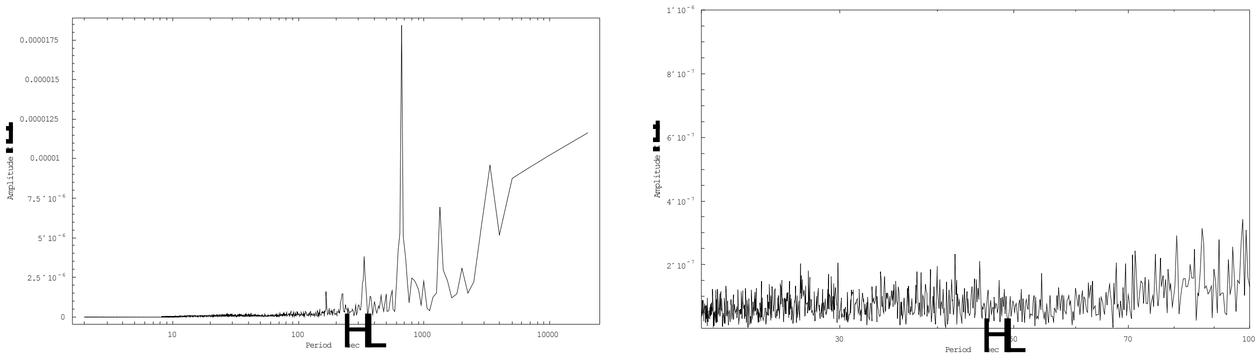

Figure 7 – Amplitude spectrum of the data stream in Figure 6. The right panel represents an expansion of the high frequency part of the spectrum

5. Estimate of the peak-to-peak effect on the final maps

In this section we show some examples of maps calculated using the time streams relative to the analyzed scenarios for all the frequency channels.

In the following figures we show maps relative to the 30, 44 and 70 GHz channels (in ecliptic coordinates) of the effect before and after classical destriping was applied. Because the classical destriping algorithm removes constant offsets from every (coadded) ring the residual effect on the destriped map is not spread uniformly over the map, but has a higher amplitude on one half of the map compared to the other. Tests are in progress using a generalised version of the destriping algorithm which is able to remove more complex functions from time ordered data (e.g. linear slopes).

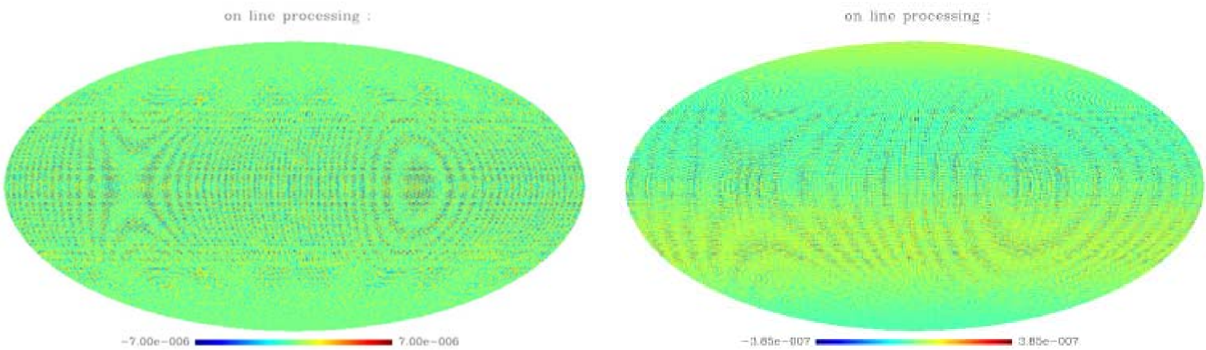

Figure 8 – Maps before (left) and after (right) destriping of the effect induced by fluctuations of the 4K reference load at 30 GHz

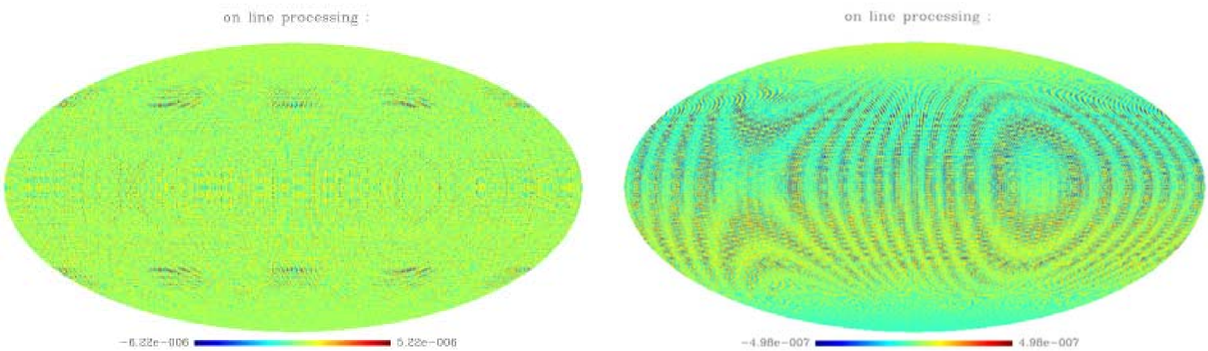

Figure 9 – Maps before (left) and after (right) destriping of the effect induced by fluctuations of the 4K reference load at 44 GHz

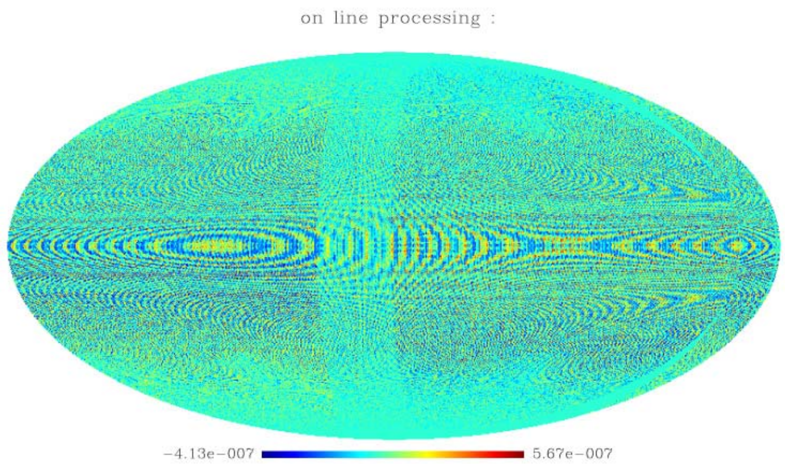

Figure 10 – Maps produced, with no destriping applied, of the effect induced by fluctuations at the interface between HFI 4K stage and the 4K reference load at 70 GHz

Table 4 - Estimated peak-to-peak effect on map with pixel sizes corresponding to the map Nside parameter

Frequency channel	30 GHz		44 GHz		70 GHz	
Pixel size (arcmin)	13.7		13.7		6.8	
	Before destriping	After destriping	Before destriping	After destriping	Before destriping	After destriping
Peak-to-peak on maps (μK)	13.68	0.75	11.44	1.01	1.01	--

6. Conclusions

In this technical note we have discussed a preliminary evaluation of the effect of temperature fluctuations in the LFI 4K reference loads on the LFI measurements. The analysis considers the expected temperature variations at the interface between the reference loads and the HFI 4K box caused by the instability of the 4K cooler cold-end driven by the 18K stage temperature fluctuations.

Temperature data measured at the LR1 cold-end on the FM2 sorption cooler have been used together with damping factors of the HFI structure calculated with the HFI thermal model; thermal dampings by the ECCOSORB loads measured during the 4K reference load QM test campaign has been used to evaluate the actual temperature fluctuation at the load extremity. The temperature variation has then been converted into antenna temperature assuming perfect emissivity in the ECCOSORB load.

The estimated signal variation at the worst case 30GHz radiometric output is of the order of ~ 0.2 mK peak to peak that translates into an error of the order of tens of micro-K per pixel when projected onto the sky. By applying classical destriping algorithms the effect is reduced to a level of the order of ~ 1 μK peak-to-peak which is close to the allowed limit in the systematic error budget plan (~ 2.2 μK peak-to-peak per pixel including spin synchronous effects).

The analysis will be soon updated with 4K reference load FM test campaign measurements and HFI new transfer functions measured during CQM test campaign.

7. References

[1] M. Seiffert, A. Mennella, C. Buriana, et al., *1/f noise and other systematic effects in Planck-LFI radiometers*, A&A, 391, 1185-1197 (2002)

[2] A. Mennella, M. Bersanelli, M. Seiffert, et al., *Offset balancing in pseudo correlation radiometers for CMB measurements*, A&A, to be published (2003)

[3] M. Bersanelli, A. Mennella, *Planck-LFI design report*, PL-LFI-PST-RP-002 3.0, March 2002

[4] M. Bersanelli, M. Seiffert, R. Hoyland, and A. Mennella, *Planck-LFI Scientific Requirements*, PL-LFI-PST-SP-011 2.0, March 2003

[5] G. Morgante, *LFI active temperature control – a first analysis*, July 2002, memo available on LiveLink at: http://www.rssd.esa.int/llink/livelink/90238/LFI_temperature_sensors_-_preliminary_overview.pdf?func=doc.Fetch&nodeid=90238

[6] L. Terenzi, *LFI PID preliminary analysis*, November 2002, memo available on LiveLink at: http://www.rssd.esa.int/llink/livelink/137034/LFI_PID_preliminary_analysis.pdf?func=doc.Fetch&nodeid=137034

[7] F. Lejdstrom, *4K thermal fluctuations and influence of a pid system v2*, TN-PH223-400507-IAS Issue 01, December 2004

[8] L.Terenzi, *Thermal test of 4K Reference Load QM targets*, PL-LFI-TES-RP-006

[9] A. Mennella, M. Bersanelli, C. Burigana, et al., *Planck: systematic effects induced by periodic fluctuations of arbitrary shape*, A&A, 384, 736-742 (2002)